ROYAL SOCIETY
OF CHEMISTRY

View Article Online

View Journal | View Issue

Check for updates

# Silver thiolate nanoclusters as support for chiral ligands: application in heterogeneous phase asymmetric catalysis†

Ludovica Primitivo, [iD] *[a] Martina De Angelis,[a] Andrea Necci,[a] Federica Di Pietro,[a] Alessandra Ricelli, [iD] [ab] Daniela Caschera, [iD] [c] Luciano Pilloni,[d] Lorenza Suber [iD] [e] and Giuliana Righi [iD] *[ab]

Silver thiolate nanoclusters have been functionalized with a chiral amino alcohol ligand that has previously shown high catalytic efficiency in different asymmetric reactions. The as-developed nano-structured catalyst, which can be easily recovered by simple centrifugation, has been tested in the addition of nitromethane to aromatic aldehydes, showing the same catalytic activity as the homogeneous ligand. Moreover, it was reused for two further recycling cycles without loss of efficiency. To the best of our knowledge, this is the first example of silver nanoclusters employed as a support for chiral ligands for heterogeneous phase asymmetric catalysis.

## Introduction

The interest in heterogeneous phase asymmetric catalysis has grown in the last few decades, thanks to the possibility of easily recovering and reusing chiral catalysts. Indeed, in homogeneous phase asymmetric catalysis, slow and expensive purification steps are usually necessary to isolate the chiral catalyst from the reaction environment, precluding the application of asymmetric catalysis in the industrial field.[1] Unfortunately, the immobilization of catalysts on solid supports often decreases the catalytic efficiency, mainly because of the poor dispersion of the support in solvents. Even soluble solid supports, like soluble polymers, have some disadvantages, such as the great dependence of the activity on the solvent and the chemical and

[a]Department of Chemistry, Sapienza University of Rome, P.le A. Moro 5, 00185 Rome, Italy. E-mail: ludovica.primitivo@uniroma1.it
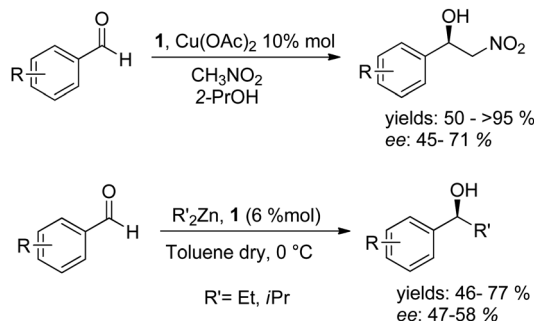
[b]CNR-IBPM-c/o Dep. Chemistry, Sapienza University of Rome, 00185 Rome, Italy. E-mail: giuliana.righi@cnr.it

[c]CNR-ISMN, Via Salaria km 29,300, 00015 Monterotondo St., Italy

[d]ENEA SSPT-PROMAS-MATPRO, Materials Technology Division, Casaccia Research Centre, 00123 Rome, Italy

[e]CNR-ISM, Via Salaria km 29,300, 00015 Monterotondo St., Italy

mechanical stability of such supports.[2,3] In this context, the use of nanoparticles could overcome these problems because, thanks to their small dimensions in the order of nanometers, they are highly dispersible in solvents and have a high surface-volume ratio that guarantees an extended functionalization with chiral catalysts.[4] All these characteristics let the nano-structured catalyst to have a catalytic efficiency comparable to that of a non-immobilized one.[5] Moreover, nanoparticles can be separated from the reaction environment using different techniques, depending on the nature of the nanoparticle itself, such as magnetic decantation or centrifugation. Many nano-structured catalysts have been developed in the last few decades, showing great catalytic efficiency and demonstrating the efficiency of this type of support.[6–9]

When the metal nanoparticle size reaches values of only a few nanometers (~2 nm) they enter the field of atomically precise nanoparticles or nanoclusters (NCs).[10] Nanoclusters are a particular class of nanoparticles which are atomically and structurally precise, with formulae of the type $M_nL_m$ (where $n$ and $m$ are integers), and many nanocluster structures have been resolved by single crystal X-ray diffraction.[11,12] Having a well-defined formula and structure, nanoclusters are also called molecular nanoparticles or nanomolecules, and are considered a bridge between molecules and nanoparticles. They are made of few $M^0$ atoms (compared to the several $M^0$ atoms of nanoparticles) that form a core, completely surrounded by metal–ligand units, that compose a shell around the core and avoid particle aggregation and coalescence phenomena.[13] Even though nanoclusters have very promising properties for heterogeneous asymmetric catalysis (e.g. excellent dispersibility, and high and reproducible functionalization), examples of their employment as supports for chiral catalysts are extremely rare and mainly with gold nanoclusters.[14–16] To the best of our knowledge, no examples of silver nanoclusters functionalized with chiral ligands have been reported so far. The choice of silver nanoclusters has some advantages with respect to that of gold ones, such as good abundance and low costs of reagents, but gold is generally preferred because of

**Scheme 1** Magnetically recoverable nanostructured catalyst **1** and its employment in asymmetric catalysis.



**Scheme 3** (a) TEPA, LiOH, THF, reflux, 12 h; (b) DIBAL, THF dry, −40 °C, 2 h, 87% from cyclohexanecarboxaldehyde; (c) TBHP, Ti(OiPr)$_4$, L-(+)-DET, DCM dry, −20 °C, 12 h, 91%, ee 97.9%; (d) TEMPO, IBDA, DCM, r.t., 2 h; (e) diethylphosphonoacetic acid, BuLi, THF dry, −70 °C− r.t., 12 h; (f) tyramine, EDC, HOBt, DMF, r.t., 12 h, 54% from **6**; (g) propargyl bromide, K$_2$CO$_3$, CH$_3$CN dry, reflux, 12 h; (h) morpholine, LiClO$_4$, CH$_3$CN dry, 55 °C, 12 h, 62% from **7**.

silver's sensitivity to air, that makes AgNCs generally less stable. However, Bigioni's group in 2013 has synthetized silver nanoclusters that are even more stable than analogous gold ones, using *p*-mercaptobenzoic acid as the ligand.[17]
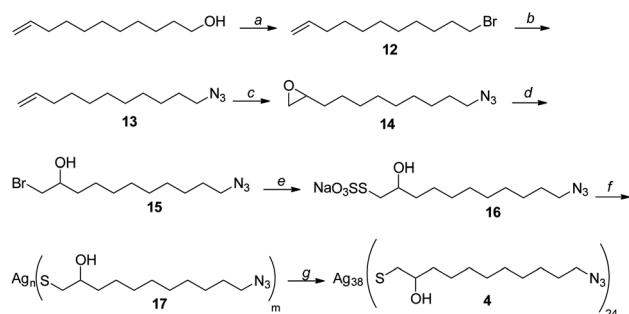
Recently we reported the employment of a magnetically recoverable nanostructured catalyst **1** in the Henry reaction and in the addition of dialkylzinc to aldehydes (Scheme 1).[18,19] In light of the great potential of silver nanoclusters, the lack of examples of their employment in heterogeneous phase asymmetric catalysis and our great experience in synthesizing these nanomaterials,[12,19–22] we considered studying their employment as a support for chiral catalysts. Herein we report the functionalization of silver nanoclusters with a chiral amino alcohol ligand and the application of the as-developed nanostructured catalyst in asymmetric catalysis.
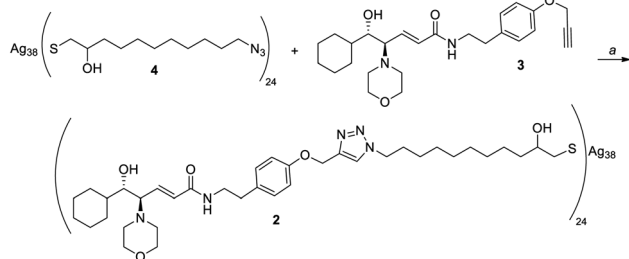
## Results and discussion

Given the high affinity of silver for sulfur and the efficiency of click chemistry as an immobilization strategy for chiral



**Scheme 2** Immobilization strategy for chiral catalyst **3** onto silver thiolate nanoclusters **4**.

catalysts, the nanostructured catalyst **2** was designed. It is derived from a click reaction between the amino alcohol ligand **3**, the same previously immobilized on magnetic nanoparticles, and the azido-functionalized silver thiolate nanoclusters **4** (Scheme 2). Nanoclusters **4** have already been extensively characterized by our group,[23] with an estimated molecular formula of Ag$_{38}$L$_{24}$ and a consequent maximum loading value of 2.4 mmol g$^{-1}$. Moreover, nanoclusters **4** were found to be easily recoverable by simple centrifugation in a proper solvent (in which the nanoclusters are less dispersible, for example THF, 2-propanol, acetone, and water).

As already reported,[18,19] ligand **3** was synthesized starting from cyclohexanecarboxaldehyde and by introducing the chirality of the molecule through a Sharpless epoxidation of allylic alcohol **5** (Scheme 3).

Silver thiolate nanoclusters **4** were instead synthesized starting with 10-undecen-1-ol, according to the synthetic pathway shown in Scheme 4. It is noteworthy that silver thiolate **17** can be reduced to obtain nanoclusters **2** using sodium ascorbate, a greener and milder reducing agent than the usually employed sodium borohydride. Synthesis of the nanoclusters **4** with the formula Ag$_{38}$L$_{24}$, with a loading of the N$_3$ functional group of 2.4 mmol g$^{-1}$, is totally reproducible. Considering that



**Scheme 4** (a) CBr$_4$, PPh$_3$, DCM, r.t., 12 h, 61%; (b) NaN$_3$, DMSO dry, r.t., 12 h, 93%; (c) oxone, NaHCO$_3$, H$_2$O/acetone, 0 °C, 2 h, 92%; (d) LiBr, Amberlyst 15, acetone, 12 h, 0 °C, 70%; (e) sodium thiosulfate, EtOH/H$_2$O reflux, 12 h, 91%; (f) AgNO$_3$, EtOH/H$_2$O, DCM; 3 h; (g) sodium ascorbate, EtOH, 70 °C, 12 h, 62%, loading 2.4 mmol g$^{-1}$.

**Scheme 5** (a) CuI (0.2 eq.), DIPEA (13 eq.), THF, r.t., 72 h, 0.13 mmol $g^{-1}$/CuI (0.2 eq.), DIPEA (1.1 eq.), THF, r.t., 72 h, 0.50 mmol $g^{-1}$/CuOAc (0.2 eq.), DIPEA (1.1 eq.), THF, r.t., 72 h, 0.43 mmol $g^{-1}$.

the latter is the moiety chosen for the immobilization of the chiral ligand, this allows great control over the functionalization of nanoclusters.

At this point, we performed the immobilization of amino alcohol **3** on nanoclusters **4** using CuI and DIPEA in THF as reaction conditions (Scheme 5). The quantitative functionalization with the chiral ligand was proven by IR analysis, which showed the complete disappearance of the intense absorption peak, at about 2100 cm$^{-1}$ due to the N=N=N stretching mode (see the ESI†), but elemental analysis of nanoclusters **2** was not comparable to that of the theoretical ones calculated considering the molecular formula (see the ESI†). In fact, the loading value was just about 0.13 mmol $g^{-1}$, lower than the theoretical one (1.2 mmol $g^{-1}$).

We hypothesized that the excess of DIPEA (13 eq.) could have interacted with the silver core, partially destroying the nanocluster structure, so we performed the reaction again using just

1.1 equivalents of the base. In this latter case nanoclusters were obtained with a higher loading (0.50 mmol $g^{-1}$), but still lower than the theoretical one.

We investigated the problem carrying out an EDS analysis on the last synthesized nanoclusters (Fig. 1), that revealed a certain amount of iodine on the nanocluster surface. We then hypothesized that the use of CuI could have led to a partial substitution of the thiolate ligand with iodine, due to the high silver affinity for halogens.

So, we changed the Cu$^{I}$ source and immobilized amino alcohol **3** on silver nanoclusters **4** using CuOAc and 1.1 equivalents of DIPEA in THF. Unfortunately, the nanostructured catalyst **2** was obtained with a slightly lower loading than the previous one, 0.43 mmol $g^{-1}$.

Then, we considered that the problem could lie in the non-optimal dispersion of nanoclusters in THF, which might have led to a partial aggregation during the reaction. So, we decided to perform the immobilization of the chiral ligand **3** on silver nanoclusters in dichloromethane, as AgNCs **4** are perfectly dispersible in this solvent. Given the lack of examples of the click reaction performed in dichloromethane, we carried out a first attempt in the homogeneous phase (Scheme 6). Azidodecane **18**, with an alkyl chain length similar to that of the thiolate ligand in nanoclusters **4**, underwent the click reaction with the amino alcohol **3** using CuOAc and 1.1 eq. of DIPEA in dichloromethane, and the reaction product **19** was obtained with an excellent yield (96%).

Employing these conditions for the functionalization of nanoclusters **4**, we finally obtained nanoclusters **2** with a loading and elemental analyses comparable to the theoretical ones (Scheme 7). This functionalization was proven to be totally
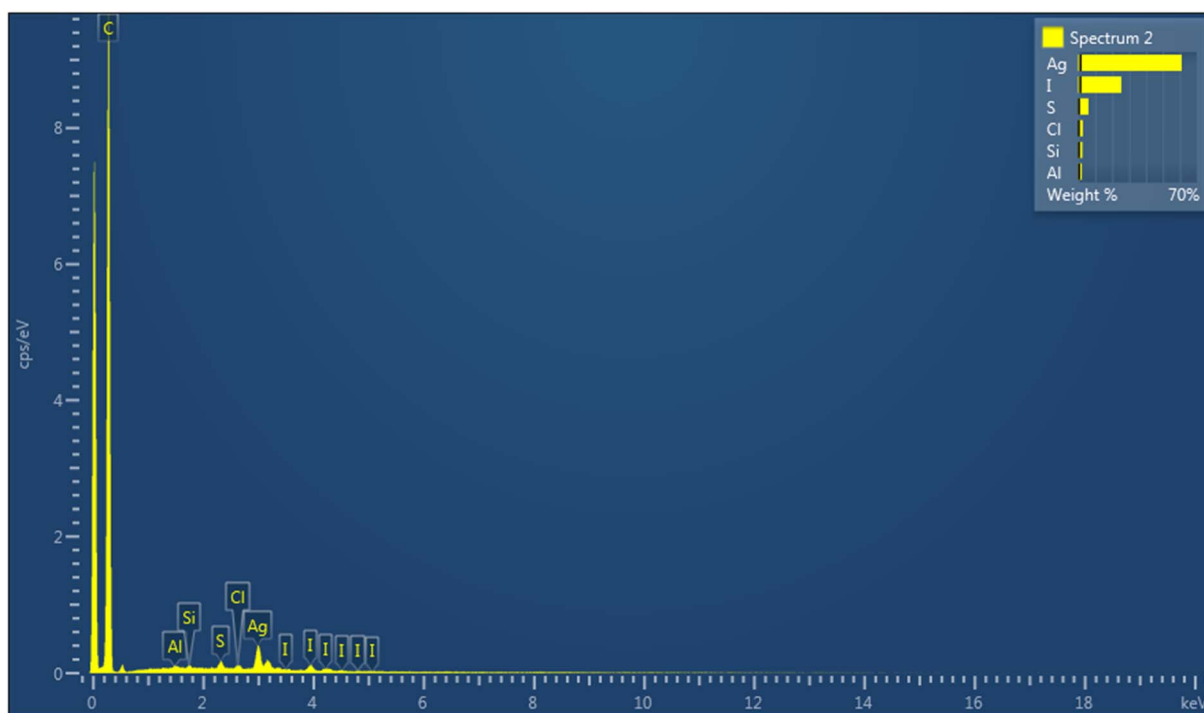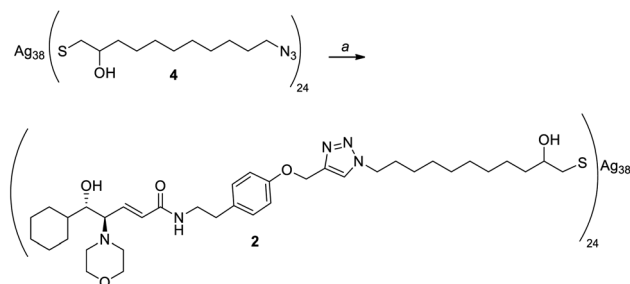


**Fig. 1** EDS spectrum of NCs **2**.
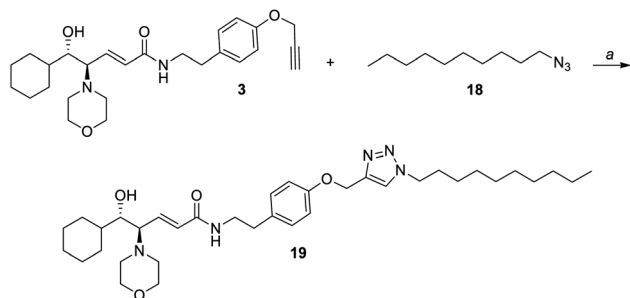
**Scheme 6** (a) CuOAc (0.2 eq.), DIPEA (1.1 eq.), DCM, 12 h, 96%.



**Scheme 7** (a) **3**, CuOAc (0.2 eq.), DIPEA (1.1 eq.), DCM, 72 h, 1 mmol g$^{-1}$.

reproducible: in fact, performing the reaction repeatedly, nanoclusters **2** were synthetized every time with the same loading and elemental analyses. Furthermore, the as-synthetized nanoclusters seemed much more dispersible in solvents than those previously obtained, supporting the hypothesis that aggregation occurred when performing the reaction in THF.

Having optimized the functionalization of nanoclusters, we moved on to the catalytic tests to evaluate the efficiency of silver

nanoclusters as a support for chiral ligands. For this purpose, we chose the Henry reaction between aromatic aldehydes and nitromethane, whereby the amino alcohol catalyst we developed showed the same catalytic efficiency in the homogeneous and heterogeneous phase (Table 1). We obtained excellent results, generally comparable to those obtained in the homogeneous phase. The *ortho*-substituted chiral benzyl nitro alcohols were obtained with a slightly lower ee with respect to the homogeneous phase, probably because of steric effects that could be enhanced in the case of immobilized ligands (Table 1, entries 6 to 8). On the contrary, in the reaction with 4-methyl-benzaldehyde the nanostructured catalyst showed a better asymmetric induction than its homogeneous counterpart, and product **20e** was obtained with a higher ee (70%) than in the homogeneous phase (63%, entry 9). Catalyst **2** also showed higher catalytic activity than the magnetically recoverable nanostructured catalyst **1** we previously reported, even though the recyclability was the same (three cycles without significant loss of activity). We also carried out the recycling tests, and the asymmetric induction of **2** has been retained for 3 catalytic cycles, while catalytic activity (in terms of yield) was maintained for all the catalytic tests performed. In the 4th and 5th cycles the asymmetric induction started to slightly decrease, probably due to aggregation phenomena. In fact, after five cycles the nano-clusters appeared less dispersed even in dichloromethane. It is, anyway, worth highlighting that, given the very high loading only a few mg of nanoclusters were necessary for catalytic tests and, given the excellent yield of recovery (around 90%) it was not necessary to conduct recycling tests scaling up the amount of catalyst with respect to the other catalytic tests. The following step will be to employ **2** in other asymmetric reactions, such as the addition of diethylzinc to aldehydes.

We also investigated the optical behavior of the NCs with and without the amino alcohol ligand, *i.e.* the nanostructured catalyst **2** and the nanocluster **4** respectively, in order to assess

**Table 1** Evaluation of the catalytic efficiency of functionalized silver–thiolate nanoclusters **2** in the Henry reaction



| Entry [a] | Substrate | Cycle | 2 | | Homogeneous ligand | | 1 | | Product |
| | | | Yield[b] (%) | ee[c] % | Yield[d] (%) | ee[c] % | Yield[d] (%) | ee[c] % | |
| --- | --- | --- | --- | --- | --- | --- | --- | --- | --- |
| 1 | Benzaldehyde | I | >95 | 66 | 86 | 68 | 81 | 67 | **20a** |
| 2 | Benzaldehyde | II | >95 | 65 | — | — | 75 | 60 | **20a** |
| 3 | Benzaldehyde | III | >95 | 65 | — | — | 73 | 60 | **20a** |
| 4 | Benzaldehyde | IV | >95 | 58 | — | — | — | — | **20a** |
| 5 | Benzaldehyde | V | >95 | 50 | — | — | — | — | **20a** |
| 6 | 2-Methylbenzaldehyde | I | 80 | 74 | 88 | 80 | 50 | 71 | **20b** |
| 7 | 2-Chlorobenzaldehyde | I | >95 | 60 | 88 | 71 | >95 | 51 | **20c** |
| 8 | 2-Methoxybenzaldehyde | I | 85 | 81 | 71 | 85 | 83 | 68 | **20d** |
| 9 | 4-Methylbenzaldehyde | I | 76 | 70 | 83 | 63 | — | — | **20e** |

[a] All the reactions were performed under identical conditions (72 h). [b] NMR yield. [c] Determined by chiral HPLC (see ESI). [d] Isolated yield.
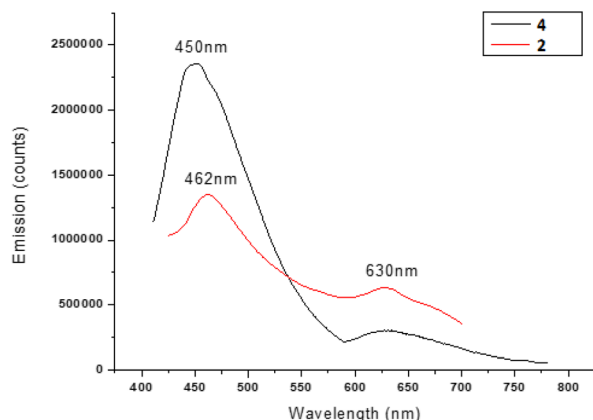
Fig. 2 Emission spectra of **2** (red line) and **4** excited at 370–400 nm.

the influence of the catalyst on the structural and physical properties of the silver nanoclusters. Unlike nanoparticles, nanoclusters, due to their hybrid metallic-molecular nature, can show fluorescence and, different from organic molecules, they can show strong and stable emissions. The emission range can reach the near infrared region, and it is very interesting especially for biomedical applications because the tissues do not absorb in this range. Both nanoclusters present bands at about 400–410 nm in UV-vis measurements (see Fig. S27 in the ESI†), as expected for silver-based materials. The steady-state fluorescence results are shown in Fig. 2. The NCs **4**, excited at 400 nm, show two emissions, in the visible region at 450 nm and at about 630 nm. Also, the NCs **2** with the ligand anchored show two emissions, one in the same position, at 630 nm, whereas the other is blue-shifted by about 12 nm to 462 nm. We can reasonably suppose that this emission could depend on the NC shell, where the peak shifting is due to the perturbation caused by the ligand anchoring. On the other hand, the emission at about 630 nm could be attributed to the NC core, which remains unperturbed. Moreover, the spectral identity and the position of the peaks in the excitation spectra (Fig. S28†), in good coherence with the absorption measurements, could confirm that no structural variation could be revealed in the nanocluster after catalyst attachment. In fact, in the case of some modification or disruption of the chemical structure, substantial changes in the excitation spectra would be expected, due to modification of fluorescence centers.

Finally it is worth noting that the presence of the amino alcohol ligand does not quench the fluorescence properties of the nanoclusters in a significant way, making them suitable for other specific applications also.

## Conclusions

Silver nanoclusters were employed for the first time as a support for chiral ligands. After an extended study aimed at optimizing the reaction conditions to immobilize a chiral amino alcohol ligand onto nanoclusters, we tested the catalytic efficiency of the chiral nanostructured catalyst **2** on the Henry reaction. All the nitro alcohol products **20** were obtained with high enantiomeric

excesses and excellent yields, generally comparable to the values obtained in the homogeneous phase. Furthermore, **2** retained its asymmetric induction for three catalytic cycles, while its catalytic activity (in terms of yield) remained unchanged for all the catalytic tests performed. Moreover, it can be easily and almost quantitatively recovered by simple centrifugation. Given the peculiar structure of nanoclusters, with a precise ratio between silver and thiolate ligands, the functionalization depends only on the NC molecular formula, and does not change from synthesis to synthesis. In addition, it has been evaluated that even in the presence of an anchored chiral ligand, the silver nanoclusters retain their fluorescence properties, showing emissions in the visible region and in the near infrared region. Interestingly, the introduction of a chiral ligand changed the emission peak in the UV-vis region. These first results show that nanoclusters are an efficient support for chiral catalysts, extending the applications of these nanomaterials to heterogeneous phase asymmetric catalysis.

## Author contributions

## Conflicts of interest

There are no conflicts to declare.

## Acknowledgements

## Notes and references

1 D. Y. Murzin, P. Mäki-Arvela, E. Toukoniitty and T. Salmi, *Catal. Rev.*, 2005, **47**, 175–256.

2 B. Altava, M. I. Burguete, S. V Luis, M. J. Vicent and J. A. Mayoral, *React. Funct. Polym.*, 2001, **48**, 25–35.

3 R. Haag, S. Roller, O. Polymerchemie and U. Dortmund, *Top. Curr. Chem.*, 2004, **242**, 1–42.

4 A. Schatz, O. Reiser and W. J. Stark, *Chem.–Eur. J.*, 2010, **16**, 8950–8967.

5 S. Roy and M. A. Pericàs, *Org. Biomol. Chem.*, 2009, **7**, 2669.

6 P. Riente, C. Mendoza and M. A. Pericás, *J. Mater. Chem.*, 2011, **21**, 7350.

7 S. M. Sarkar, M. E. Ali, M. L. Rahman and M. Mohd Yusoff, *J. Nanomater.*, 2015, **2015**, 1–6.

8 A. Hu, G. T. Yee and W. Lin, *J. Am. Chem. Soc.*, 2005, **127**, 12486–12487.

9  J. Li, Y. Zhang, D. Han, Q. Gao and C. Li, *J. Mol. Catal. A: Chem.*, 2009, **298**, 31–35.

10  X. Huang, Z. Li, Z. Yu, X. Deng and Y. Xin, *J. Nanomater.*, 2019, **2019**, 1–31.

11  R. Jin, C. Zeng, M. Zhou and Y. Chen, *Chem. Rev.*, 2016, **116**, 10346–10413.

12  P. N. Gunawardene, J. F. Corrigan and M. S. Workentin, *J. Am. Chem. Soc.*, 2019, **141**, 11781–11785.

13  L. Suber, P. Imperatori, L. Pilloni, D. Caschera, N. Angelisi, A. Mezzi, S. Kaciulis, A. Iadecola, B. Joseph and G. Campi, *Nanoscale*, 2018, **10**, 7472–7483.

14  K. Marubayashi, S. Takizawa, T. Kawakusu, T. Arai and H. Sasai, *Org. Lett.*, 2003, **5**, 4409–4412.

15  S. Takizawa, M. L. Patil, K. Marubayashi and H. Sasai, *Tetrahedron*, 2007, **63**, 6512–6528.

16  T. Belser and E. N. Jacobsen, *Adv. Synth. Catal.*, 2008, **350**, 967–971.

17  A. Desireddy, B. E. Conn, J. Guo, B. Yoon, R. N. Barnett, B. M. Monahan, K. Kirschbaum, W. P. Griffith, R. L. Whetten, U. Landman and T. P. Bigioni, *Nature*, 2013, **501**, 399–402.

18  C. Sappino, L. Primitivo, M. De Angelis, M. O. Domenici, A. Mastrodonato, I. Ben Romdan, C. Tatangelo, L. Suber, L. Pilloni, A. Ricelli and G. Righi, *ACS Omega*, 2019, **4**, 21809–21817.

19  C. Sappino, L. Primitivo, M. De Angelis, F. Righi, F. Di Pietro, M. Iannoni, L. Pilloni, S. V. Ciprioti, L. Suber, A. Ricelli and G. Righi, *RSC Adv.*, 2020, **10**, 29688–29695.

20  D. C. L. Suber, L. Pilloni, K. Khanna, G. Righi, L. Primitivo and M. De Angelis, *J. Nanosci. Nanotechnol.*, 2021, **21**, 2816–2823.

21  L. Suber and W. R. Plunkett, *Nanoscale*, 2010, **2**, 128–133.

22  A. Mari, P. Imperatori, G. Marchegiani, L. Pilloni, A. Mezzi, S. Kaciulis, C. Cannas, C. Meneghini, S. Mobilio and L. Suber, *Langmuir*, 2010, **26**, 15561–15566.

23  G. Campi, L. Suber, G. Righi, L. Primitivo, M. De Angelis, D. Caschera, L. Pilloni and A. Del, *Nanoscale Adv.*, 2021, **3**, 2948–2960.